Functional Materials 20, No.1 (2013)

Indium induced nanostructures on In_4Se_3(100) surface studied by scanning tunneling microscopy

P.V.Galiy, T.M.Nenchuk, A.Ciszewski*, P.Mazur*, S.Zuber*, Ya.M.Buzhuk

Electronics Department, I.Franko Lviv National University,
79005 Lviv, Ukraine
*Institute of Experimental Physics, University of Wroclaw,
50-204 Wroclaw, Poland

Received September 12, 2012

Indium deposition leads to changes in the scanning tunneling microscopy (STM)-revealed (100) surface morphology of In_4Se_3 layered semiconductor with the formation of nanostructures, which are characterized by different dimensionality dependent on different crystal growth conditions. Preferable formation of nanodots in low and quasi one dimensional (1D) structures for the high bulk-conductivity crystals has been observed. The STM and scanning tunneling spectroscopy data enable us to consider that the dimensionality, shape and direction of the obtained indium deposition structures are induced by indium clusters available on the original, on-the-lattice-scale furrowed, ultra high vacuum (UHV) (100) cleavages of In_4Se_3 crystal due to the self-intercalation phenomenon.

Напыление индия приводит к изменениям морфологии поверхности (100) слоистого кристалла In_4Se_3, которые наблюдаются с помощью сканирующей туннельной микроскопии (СТМ), с формированием наноструктур разной размерности, зависящей от условий выращивания кристаллов. Наблюдается превалирующее формирование наноточек для кристаллов с низкой и квази одномерных структур для кристаллов с высокой проводимостью. Данные СТМ и сканирующей туннельной спектроскопии позволяют сделать заключение о том, что размерность, форма и направление полученных напыленных индиевых структур обусловлены кластерами индия, которые присутствуют на исходной поверхности (100) сверхвысоковакуумных сколов кристаллов In_4Se_3 вследствие явления самоинтеркаляции.

1. Introduction

Studies of surface self-assembling structures directed by a variety of templates are still of relevance to yield functional nanostructures e.g. nanowires and an organized array of nanodots [1, 2]. From this point of view (100) surface of layered semiconductor crystals In_4Se_3 can act as a natural template [3] for growing various low dimensional structures due to their intrinsic bulk anisotropy [4, 5], that allows to obtain cleavages with the chainlike-furrowed structure on the nanoscale [6].

Regarding the (100) surface morphology of In_4Se_3 the presence of stair-like superstructure with nanowire-like cylindrical clusters of diameter about 20 nm and stairs in the cleavage plane up to 5 nm, which depends on the cleavage conditions, has been reported in [7].

The present work concerns with scanning tunneling microscopy/scanning tunneling spectroscopy (STM/STS) study of the (100) cleavage surface morphology of In_4Se_3 lay-

ered semiconductor crystals with self-assembled indium nanostructures obtained under different growth conditions.

2. Experimental

In_4Se_3 crystals grown by Czochralski method from In_4Se_3 with up to 10 atomic percent In alloy were *n*-doped by In with a carrier concentration of $10^{15}/10^{19}$ cm^{-3} (as measured at 0.01/0.11 $(Ohm \cdot cm)^{-1}$ the low/high conductivity, respectively).

STM/STS data were obtained at room temperature with an Omicron NanoTechnology STM/AFM System under ultra high vacuum (UHV) conditions ($4 \cdot 10^{-9}$ Pa) from *in situ* crystal cleavages. Specimens for STM studies had dimensions 3×4×6 mm^3 and special shape suitable for multiple cleavages *in situ*. The STM images were acquired in the constant current mode. The STS was used in the current imaging tunneling spectroscopy (CITS) mode. Indium was evaporated from an Omicron EFM3 system. The ion current inside the effusion cell was controlled to be constant during the indium deposition. The crystals were annealed after growth during 12 h as well as after indium deposition (0.5 h) at 575 K. To visualize the measured STM/STS data we employed WSxM software v.4.0 designed by Nanotec Electronica [8].

3. Results and discussion

3.1. Study of the initial surfaces

The orthorhombic layered crystals of In_4Se_3 can be cleaved perfectly along the (100) plane to expose macroscopic flat regions [6], although STM study yields a furrowed lattice relief [9]. The furrows have the structure with **c** and **b** periodicity, respectively, along and normal to them, in accordance with the crystallography (**c** = 4.08 Å, **b** = 12.3 Å) [4]. However, the STM images of (100) surface for In_4Se_3 crystals with the high conductivity, in contrast to those with the low one, are usually more noisy. It is often difficult to get a clear lattice periodicity for them, even with a two dimensional fast Fourier transform (2D FFT) filtering application. In view of the STS study described below, this result could be explained by the presence of high concentrations of self-intercalated indium on (100) surface of In_4Se_3 crystals with the high bulk conductivity.

Fig. 1a shows an STM image of the UHV cleavage (scan size 150×150 nm^2) of the low conductivity crystal In_4Se_3 before indium deposition. The on-a-macroscale smooth cleavages often exhibit growth striped structures along **c**-axis, easily observed even by optical methods. A segment of such structure can be seen in Fig. 1a (upper left corner). Fig. 1b shows the FFT filtering of the image, which reveals a periodical structure co-directed to the growth striped one with a subsequent profile (Fig. 1d) that gives the lattice periodicity along **b** direction, well-consistent with that of bulk, 1.25 nm. The fragment of crystal structure [4] with a triangle indicating the cleavage direction and, consequently, the interlayer (100) cleavage plane is shown in Fig. 1c. The **c**-axis oriented growth of nanosized clusters on In_4Se_3 (100) surfaces was also reported previously [7].

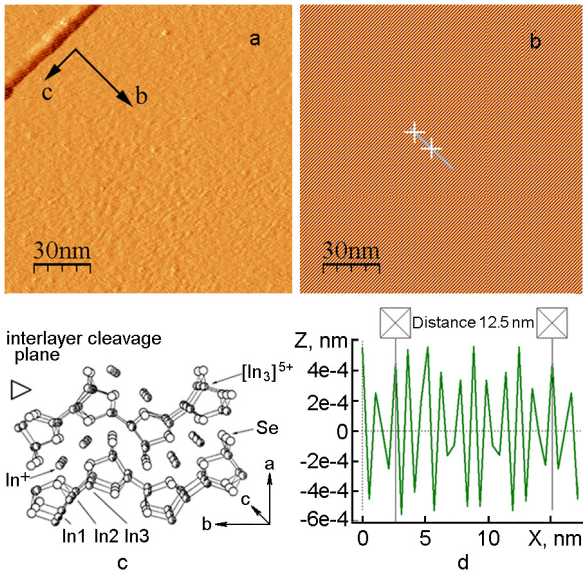

Fig. 1. STM image of the UHV In_4Se_3(100) cleavage (scan size 150×150 nm^2, sample bias 1.2 V, tunneling current 86 pA) of the low conductivity In_4Se_3 crystal before indium deposition: (a) Growth "protrusion" as shown in the upper left corner, **b** and **c** mark the bulk lattice directions in the cleavage plane; (b) Image after FFT with the subsequent profile shown in (d) that gives the lattice periodicity along **b** direction (well-consistent with that of bulk, 1.23 nm); (c) In_4Se_3 structure fragment (projection on (001) plane) [4] with triangle indicating the cleavage plane (100).

Actually the large-scale STM surface morphology images often exhibit well-resolved natural nanostructures. The STM image in Fig. 2 shows a UHV cleavage surface (scan size 3×3 μm^2) of In_4Se_3 high conductivity crystal before indium deposition, with natural nanostructures (a) and subsequent profile (b).

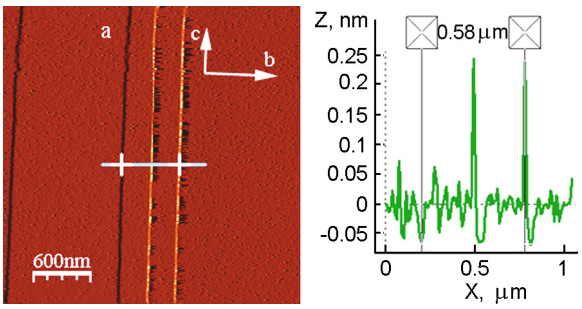

Fig. 2. (a) STM image of the UHV In_4Se_3(100) cleavage (scan size 3×3 μm^2, sample bias 1.7 V, tunneling current 105 pA) of the high conductivity In_4Se_3 crystal before indium deposition, with natural nanostructures. (b) The subsequent profile in *b* direction.

STS spectra of the studied initial surfaces with "flat" regions indicate a value of 0.68 eV for the energy gap, already derived for bulk crystal [10]. Fig. 3 shows typical averaged STS spectra of the initial UHV cleavages (scan size 50×50 nm^2) of In_4Se_3 crystals with low (1) and high (2) conductivity.

3.2. Indium deposited surfaces

Studies of the self-assembled structures formation during metal deposition on the initially smooth surfaces of layered compounds are of interest due to the quasi-two-dimensional character of the structures giving rise to unique electronic properties [11, 12]. Particularly, an influence of the copper intercalation into a thin surface layer on nanostructure formation was studied [13]. It is well known that electronic properties of layered crystals can be modified in a controlled way by intercalating various guest species into the interlayer space [14]. We observed the existence of induced nanophases for (100) surfaces of In_4Se_3 crystals intentionally intercalated by copper during the crystal growing [15]. Indium as the metal for deposition onto In_4Se_3 cleavage surface was selected in this work due to the evident existence of an indium wetting layer on the surface. Unlike the intercalation of copper during the crystal growth, that of indium looks like a commonly observed natural process. The amount of overstoichiometric indium that dopes the crystal can be controlled by the growing conditions and, consequently, due to the self-intercalation process, indium appears in the interlayer gap, that results in its final concentration on the cleavage surface. The presence of localized indium clusters on the UHV (100) cleavages of In_4Se_3 before the

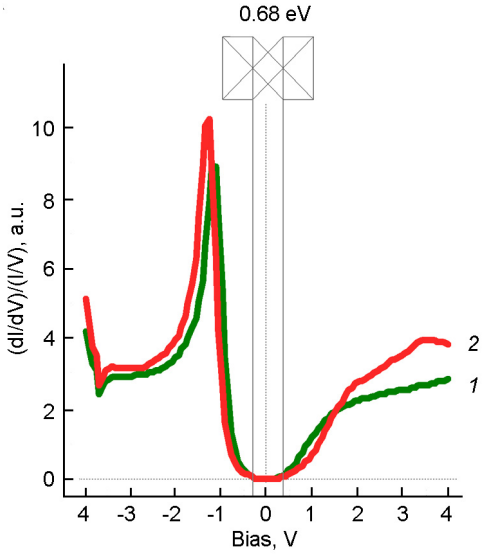

Fig. 3. Typical averaged STS spectra (6400 image points) of the initial UHV (100) cleavages (scan size 50×50 nm^2) of In_4Se_3 crystals with low (*1*) and high (*2*) conductivity.

deposition has been clearly detected by our STS study (one could find the final density of states in the energy gap of semiconductor, see below).

Indium *in situ* deposition onto UHV (100) cleavages of In_4Se_3 leads to changes in the STM-revealed surface morphologies, which are unexpectedly different for the crystals surfaces with different bulk conductivity. To quantify the deposited In nanostructures, the STM data were analyzed by averaging the roughness of 1×1 μm^2 area for different random positions on the surface to minimize an influence of local topography variations. The roughness analysis was performed for the images with the same value and polarity of bias voltage. We estimated In deposition rate by referring to the averaged height via the evaporation time curves obtained by means of roughness analysis of the covered surfaces. The roughness analysis allows to define the quantity of deposited In in pixels or dots of STM image related to the appropriate height intervals. Actually, this quantity represents the value of corresponding areas of the STM image when multiplied by area of one pixel. The product of thus determined area and corresponding height gives the volume of deposited In and the sum of all such defined volumes divided by the total image area represents the averaged height of deposited indium layer. Thus, the slope of the average

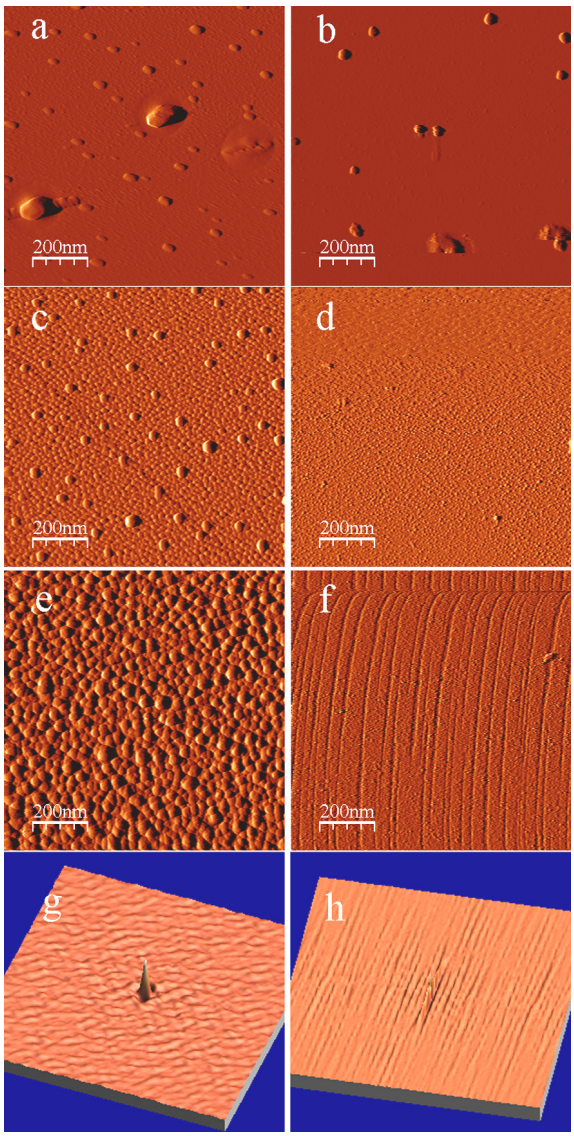

Fig. 4. STM images of the UHV (100) cleavages (scan size 1×1 μm^2, sample biases between 1.6 and 1.7 V, tunneling current ≅100 pA) of the low (figures a, c, e) and high (figures b, d, f) conductivity In_4Se_3 crystals after 35, 215, 480 seconds of In deposition. (g, h) Corresponding 3D images of self-correlation filtering of (e, f) images.

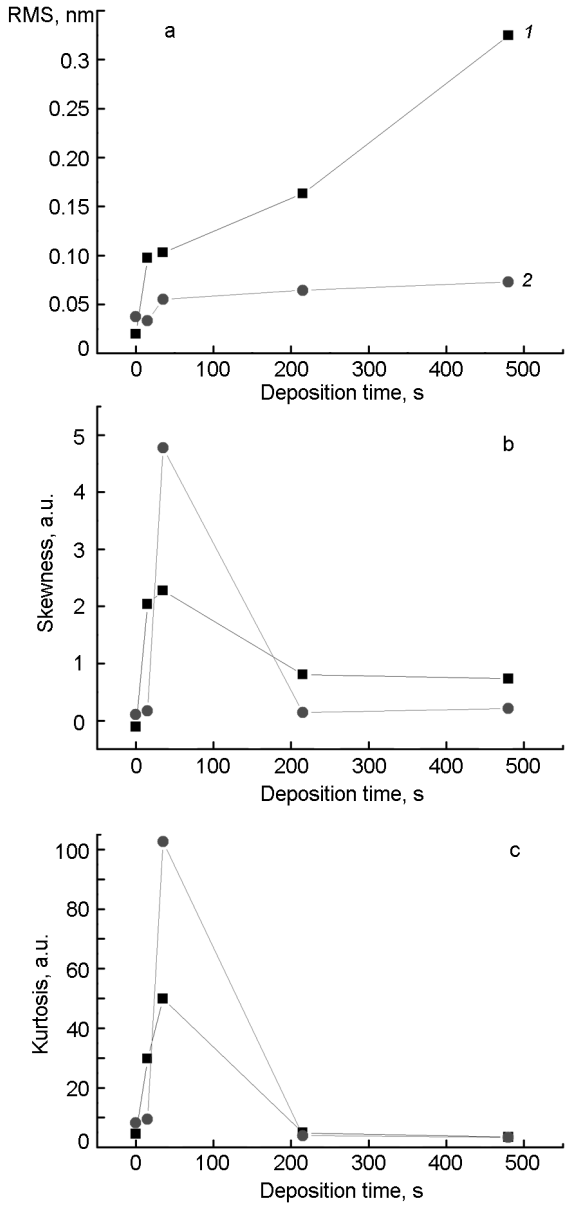

Fig. 5. (a) RMS roughness of 1×1 μm^2 areas on In_4Se_3(100) surfaces calculated from STM topographies taken at similar deposition times for the low (*1*) and high (*2*) conductivity bulk crystals. Diagrams (b) and (c) show the corresponding data of skewness and kurtosis analyses, respectively.

height via the deposition time graph defines the indium deposition rate.

The values of indium deposition rate for the high and low conductivity crystals amount to about 3×10^{-4} nm/s. The morphologies of In deposition structures on the low (Figs. 4a, c, e) and high (Figs. 4b, d, f) bulk conductivity In_4Se_3 substrates with the same In depositions are illustrated by the 1×1 μm^2 STM images, thus, being concentration and crystal growth-conditions dependent.

Figs. 4g, h show the self-correlation filtering results of the images presented in Figs. 4e, f, respectively. Any periodicity in the original STM image could be shown as a periodic pattern in the 2D self-correlation. The apparent periodical structures for the high conductivity bulk crystal surfaces (see Fig. 4h) show a relatively high degree of

order with a 25 nm periodicity. The preferable formation of nanodots (0D structures) for high resistivity (Fig. 4g) and quasi 1D structures for low-resistivity (Fig. 4h) samples is observed.

Obviously, the root-mean-square (RMS) roughness of the surface (100) of In_4Se_3 increases with the amount of indium deposition (see Fig. 5a). The surface skewness analysis (Fig. 5b) indicates lowering of the surface skewness during deposition, which indicates the appearance of almost the same number of the self-like shaped high and low areas for the highly indium covered surfaces. During the first stages of indium deposition high clusters distant from one another are formed on $In_4Se_3(100)$ surface, then the more tight cluster structure appears. However, the skewness and especially RMS for the highly indium covered surfaces of the high conductivity samples have sufficiently smaller values than those of the low conductivity ones, which indicates a relatively different formation of surface nanostructures. Also kurtosis analysis (Fig. 5c) indicates a somewhat more mean peakedness for the highly In deposited surfaces of the low conductivity In_4Se_3 crystals unlike for high conductivity ones.

The relatively higher values of skewness and kurtosis in the case of high conductivity rather than low conductivity crystals for small values of coverage (about 50 s of deposition) are associated with the presence of more quantity self-like shaped pixels in a STM image with a certain height. This confirms the existence of more nuclei of a new phase (indium clusters) on the surfaces of high conductivity crystals due to indium selfintercalation. The following behavior of skewness and kurtosis, when their values for the low conductivity of crystals become larger than that for high conductivity ones, is caused by switching from 0D to 1D dimensional nanostructures formation in the last case.

To summarize, the results presented here can be divided in two parts. It is clear that In islands nucleate preferentially on particular areas of the cleavages of $In_4Se_3(100)$ at short deposition times. Second, the reported indium growth on the surface switches from 0D to 1D mode depending on bulk conductivity of the samples, which makes it potentially suitable to control the nanostructures formation.

3.3. Spatially resolved STS study

The differences in STM morphology become clear after application of spatially resolved STS to study $In_4Se_3(100)$ substrates. Apparently, the driving force for the deposited nanostructures dimensionality is the over-stoichiometric indium being available on the initial cleavage surfaces due to the self-intercalation phenomenon. Obviously, intercalation leads to the charge transfer between intercalate and the layered crystal. Indium intercalate in In_4Se_3 crystals is defined as a donor according to the direction of Fermi level displacement [16]. Thus, availability of intercalated indium into the

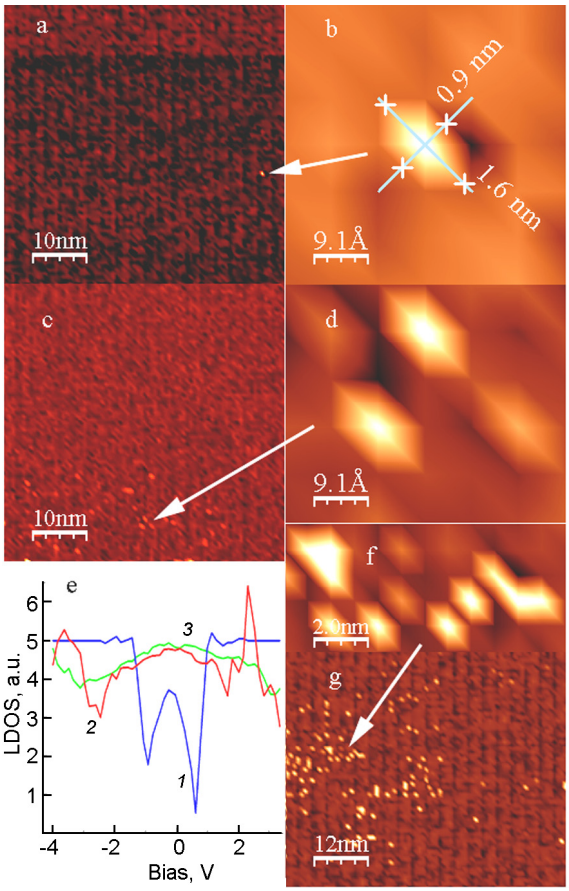

Fig. 6. STM results. The images of the UHV (100) In_4Se_3 crystal cleavages (sample bias −28 mV): (a, c) of the low/high conductivity ones before indium deposition (scan size 52×52 nm^2) and (g) of the low conductivity one (scan size 60×60 nm^2) after 15 sec In deposition with (b, d, f) indicated enlarged fragments, respectively. (e) STS results. Local density of states derived from spatially resolved STS data for local protrusions on In_4Se_3 surfaces, as observed on 6a, c, g: curve (*1*) — low conductivity crystal after 15 sec In deposition, curve (*2*) — high conductivity crystals before In deposition, curve (*3*) — low conductivity crystals before In deposition.

interlayer space results in the value of bulk conductivity and, consequently, indium presence on the (100) cleavage surfaces of In_4Se_3 should be reflected in the electron tunneling process.

Figs. 6a, c, g show the STM images of the UHV (100) cleavages (bias −0.028 V) of In_4Se_3 low/high conductivity crystals before indium deposition and low conductivity one after 15 sec of In deposition, respectively, extracted from the CITS data with subsequent enlarged fragments of protrusions (Figs. 6b, d, f). The STM images were obtained with rather a low bias voltage compared with the approximately 0.67 eV of the band gap for In_4Se_3. STM images with so low imaging bias may arise from the existence of a certain doping density inside the grown crystals, which usually are of *n*-type and also can be *p*-type or compensated semiconductors.

The CITS data allow us to associate the electronic properties combined with spatial information by extracting the images in −4 V to +4 V range of biases and application of multiple profiling. The local density of states (LDOS) vs. bias voltage as derived from the spatially resolved STS data for "protrusions", acquired from a software colour table, (such as in Fig. 6a, c, g) on the surfaces of In_4Se_3 crystals with different values of bulk conductivity, before and after indium deposition, are presented in Fig. 6e.

The local electronic structures confirmed by STS spectra in Fig. 6e are characteristic of thin metallic overlayers on the semiconductor substrates [17]. This suggests that the modulation arises from indium clusters localized at the furrowed of In_4Se_3 (100) surface relief.

Figs. 6b, d, f shows that the electronically modulated regions are localized at elongated clusters. The size and shape of these clusters are similar in the case of the low and high conductivity crystals for initial surfaces before deposition and commonly for the low indium deposited ones. Moreover, the comparison of Figs. 6a and c suggests that concentration of clusters at the initial (100) surfaces of In_4Se_3 is actually different for low/high conductivity crystals, confirming indium selfintercalation in the interlayer gap and thus its appearance on the cleavage surfaces.

One could consider that elongated shape and size of these clusters might be due to the nature of their formation through the localization to the furrowed cleavage surface's structure of In_4Se_3 crystals along **c** direction. In addition to such surface relief, it may have an impact on this localization a proper arrangement of In^+ atoms, shown in projection of In_4Se_3 crystal structure on (001) plane [4] (see Fig. 1), which are very weakly connected to the rest of the atoms.

Besides, Figs. 6d, f show the periodicity of such clusters location in the direction normal to their longer side, which is commensurate with the lattice period along the direction **b** of crystal.

Thus, indium clusters, available on the initial In_4Se_3(100) surfaces in concentrations dependent on crystal growth conditions and which are placed in specific locations of the surface structure, act as the nucleation sites of a new indium phase which is formed on the cleavages in the process of indium deposition by evaporation.

4. Conclusions

We have observed by STM the different morphologies of the surfaces In_4Se_3(100) with indium deposition obtained due to In concentration dependent bulk-crystal growing conditions. The surface roughness and 2D self-correlation analysis confirm the preferable formation of nanodots at low conductivity and 1D structures, for the high conductivity samples. Therefore, controlling the initial In_4Se_3 bulk conductivity is probably the first step of establishing the dimensionality of deposited indium nanostructures. The spatially resolved STS data enable us to consider that the shape and direction of the observed indium deposition structures are induced by the presence of indium clusters on the initial In_4Se_3(100) crystal substrates due to the self-intercalation phenomenon.

References

1. P.Kumar, *Nanoscale Res. Lett.*, **5**, 1367 (2010).
2. N.Wang, Y.Cai, R.Q.Zhang, *Mater. Sci. and Engin.*, **R 60**, 1 (2008).
3. P.V.Galiy, A.Ciszewski, O.R.Dveriy et al., *Functional Materials*, **16**, 279 (2009).
4. U.Schwarz, H.Hillebrecht, H.J.Deiseroth, R.Walther, *Zeitschrift fur Kristallographie*, **210**, 342 (1995).
5. J.-S.Rhyee, K.H.Lee, S.M.Lee et al., *Nature*, **459**, 965 (2009).
6. Ya.B.Losovyj, Melanie Klinke, En Cai et al., *Appl. Phys. Lett.*, **92**, 122107 (2008).
7. O.A.Balitskii, V.P.Savchyn, B.Jaeckel, W.Jaegeremann, *Physica E*, **22**, 921 (2004).
8. I.Horcas, R.Fernandez, J.M.Gomez-Rodriguez et al., *Rev. Sci. Instrum.*, **78**, 013705 (2007).

9. P.V.Galiy, T.M.Nenchuk, O.R.Dveriy et al., *Chem. Metals and Alloys*, **4**, 1 (2011).
10. M.Sznajder, K.Z.Rushchanskii, L.Yu.Kharkhalis, D.M.Bercha, *Phys. Stat. Sol.(b)*, **243**, 592 (2006).
11. R.Adelung, F.Ernst, A.Scott et al., *Adv. Matter.*, **14**, 1056 (2002).
12. P.Schmidt, J.Kroger, B M.Murphy et al., *New J. Phys.*, **10**, 013022 (2008).
13. E.Spiecker, A.Schmid, A.Minor et al., *Phys. Rev. Lett.*, **96**, 086401 (2006).
14. W.R.McKinnon, R.R.Haering, Physical Mechanisms of Intercalation in Modern Aspects in Electrochemistry, ed. by R.E.White, J.O'M.Bockris, B.E.Conway, Plenum Press, New York (1983).
15. P.V.Galiy, A.V.Musyanovych, Ya.M.Fiyala, *Physica E*, **35**, 88 (2006).
16. L.S.Demkiv, T.M.Demkiv, V.P.Savchyn, J.M.Stakhira, *J. Phys. Stud.*, **2**, 536 (1998).
17. R.Wiesendanger, Scanning Probe Microscopy and Spectroscopy: Methods and Applications, Cambridge University Press, Cambridge, UK (1994).

Дослідження методом скануючої тунельної мікроскопії індієвих наноструктур на поверхні (100) кристала In_4Se_3

П.В.Галій, Т.М.Ненчук, А.Ціжевський, П.Мазур, С.Жубер, Я.М.Бужук

Напилення індію приводить до змін морфології поверхні (100) шаруватого напівпровідника In_4Se_3, що спостерігаються за допомогою скануючої тунельної мікроскопії (СТМ), з формуванням наноструктур різної розмірності, яка залежить від умов вирощування кристалів. Спостерігається переважаюче формування наноточок для кристалів з низькою і квазіодномірних структур для кристалів з високою провідністю. Дані СТМ і скануючої тунельної спектроскопії дозволили зробити висновок, що розмірність, форма і напрям отриманих напилених індієвих структур обумовлені кластерами індію, які є наявними на вихідній поверхні (100) надвисоковакуумних сколів кристалів In_4Se_3 внаслідок явища самоінтеркаляції.